Biosensors and Bioelectronics 51 (2014) 268–273

Contents lists available at ScienceDirect

Biosensors and Bioelectronics

journal homepage: www.elsevier.com/locate/bios

Potentiometric glucose biosensor based on core–shell Fe_3O_4–enzyme–polypyrrole nanoparticles

Zhengpeng Yang [a,b,*], Chunjing Zhang [a], Jianxin Zhang [a], Wanbei Bai [c]

[a] Institute of Materials Science and Engineering, Henan Polytechnic University, Jiaozuo 454000, China
[b] Cultivating Base for Key Laboratory of Environment-friendly Inorganic Materials in University of Henan Province, Henan Polytechnic University, Jiaozuo 454000, China
[c] Institute of Resources and Environment, Henan Polytechnic University, Jiaozuo 454000, China

ARTICLE INFO

Article history:
Received 7 April 2013
Received in revised form
16 July 2013
Accepted 21 July 2013
Available online 6 August 2013

Keywords:
Fe_3O_4–enzyme–Ppy
Magnetic immobilization of enzyme
Magnetic electrode
Glucose oxidase
Potentiometric biosensing

ABSTRACT

Core–shell Fe_3O_4–enzyme–polypyrrole (Ppy) nanoparticles with excellent magnetism and conductivity were successfully prepared via the surface modification and enzyme self-encapsulation within Ppy. A novel potentiometric glucose biosensor has been constructed by effectively attaching the proposed Fe_3O_4–enzyme–Ppy nanoparticles to the surface of the magnetic glassy carbon electrode (MGCE). The optimum biosensing conditions could be provided with polymerization time of pyrrole for 6 h and 0.42 mg immobilization amount of Fe_3O_4–enzyme–Ppy nanoparticles on MGCE. The performance of the developed glucose biosensor was evaluated and the results indicated that a sensitive glucose biosensor could be fabricated. The obtained glucose biosensor presents shorter response time (6 s), wider linear range (0.5 μM to 34 mM), lower limit of detection (LOD, 0.3 μM), high-selectivity monitoring of glucose and good stability (with about 98.1% of the initial response signal retained after 20 days). The analytical application of the glucose biosensor confirms the feasibility of glucose detection in serum sample.

1. Introduction

Enzyme biosensors have attracted much attention in recent years due to their potential applications in clinical diagnostics, pharmaceutical, environmental analysis and food industry (Wang et al., 2008; Kotanen et al., 2012; Snyder et al., 2011). The effective immobilization of enzyme is the key step in constructing a biosensor. Various techniques have been developed for enzyme immobilization on solid surfaces, such as electrodeposition (Tan et al., 2010), self-assembly (Kim et al., 2011; Liang et al., 2013), dip coating (Pang et al., 2009), electropolymerization (Kotanen et al., 2013), polymer entrapment (Zhao and Ju, 2006), covalent attachment (Hrapovic et al., 2004) and sol–gels (Pasunooti et al., 2010). Despite many advances in enzyme biosensors, it is still a challenge to search for some new materials and methods to improve the simplicity, sensitivity, selectivity and stability of the biosensors.

Magnetic nanoparticles as special biomolecule carriers are of current interest in bio-applications such as biomedicine (Zhao et al., 2006), immunology (Vijayalakshmi et al., 2008), biocatalysis (Wei and Wang, 2008) and separation/purification of biomolecules (Kim et al., 2007) due to their biocompatibility, less toxicity, high specific surface area and strong magnetic properties. The enzymes have also been successfully immobilized onto magnetic nanoparticles modified by ionic liquids (Zhou et al., 2012), chitosan (Zhang et al., 2010), gum Arabic (Mahmood et al., 2013), carboxyl (Guo et al., 2012), gold (Kalska-Szostko et al., 2012), silica (Wu et al., 2011) and carbodiimide (Jordan et al., 2011). Among them, the method involving binding via carbodiimide activation has increased in popularity and is notable due to its simplicity and high efficiency (Chen and Liao, 2002). However, the expected high stability and activity of enzymes can not be still met due to the loss of enzymatic functions (Xia and Ma, 2010; Jordan et al., 2011). The encapsulation of enzyme molecules provides an efficient route to inhibit enzyme inactivity (Yang et al., 2008). The enzymes have been encapsulated within nanogel, Ppy and organic/inorganic network, showing a significantly enhanced stability and activity (Kim and Grate, 2003; Ramanavičius et al., 2005, 2012; Yan et al., 2006; Zou et al., 2010).

The MGCE supplies a simple, effective and inexpensive way to immobilize proteins, and is promising for construction of biosensors (Peng et al., 2011a, 2011b; Qiu et al., 2010). MGCE modified by core–shell molecularly imprinted polymer has also been used as selective sensor for metronidazole determination (Chen et al., 2013). Recently, a high performance biosensor has been constructed by effectively attaching the proposed glucose oxidase–Au–polydopamine–Fe_3O_4 magnetic bionanoparticles to the surface of the MGCE (Peng et al., 2013).

In the present work, combining the advantages of superparamagnetism from Fe_3O_4 nanoparticles and high stability from

* Corresponding author at: Henan Polytechnic University, Institute of Materials Science and Engineering, No. 2001, Century Avenue, Jiaozuo 454000, China. Tel.: +86 0391 3983800.
E-mail address: zhengpengyang@yahoo.com.cn (Z. Yang).

0956-5663/$ - see front matter © 2013 Elsevier B.V. All rights reserved.
http://dx.doi.org/10.1016/j.bios.2013.07.054

enzyme within conductive Ppy, core–shell Fe_3O_4–enzyme–Ppy nanoparticles have been prepared and a novel potentiometric biosensor has been developed for the determination of glucose based on the modification of Fe_3O_4–enzyme–Ppy nanoparticles onto MGCE through magnetic immobilization. The constructed biosensor shows excellent performance for glucose determination.

2. Experimental

2.1. Materials and apparatus

Glucose oxidase (GOD, EC 1.1.3.4, Type II, 200 U mg^{-1}, from Aspergillus niger) and 1-ethyl-3-(3-dimethyl amino propyl) carbodiimide hydrochloride (EDC) were purchased from Sigma Chem. Co. and used as received. Pyrrole monomer was obtained from Merck and distilled before use. Glucose was supplied by Sinopharm Chemical reagent Co., Ltd.. All other chemicals were of analytical grade and used without further purification. Deionized (DI) water (resistivity of 18 MΩ cm) was obtained from a Millipore Milli-*Q* Water System (Millipore Inc.), and was used for rinsing and for makeup of all aqueous solutions.

A Gamry potentiostat (model 600, USA) in a conventional three-electrode arrangement equipped with a glassy carbon working electrode, a platinum wire counter electrode and an Ag/AgCl reference electrode was employed to perform electrochemical studies. Transmission electron microscope (TEM) image was obtained at 120 kV on a Hitachi model H-800 transmission electron microscope. Infrared (IR) spectra were recorded on Nicolet 200SXV Fourier transform infrared (FTIR) spectrometer using a KBr wafer. The magnetization measurements were carried out using model 155 vibrating magnetometer. The conductivity of Fe_3O_4–GOD–Ppy nanoparticles at room temperature was measured by the conventional four-point probe technique with a digital multimeter and a programmable dc voltage/current source on compressed pellets of dried powders.

2.2. Preparation of Fe_3O_4–GOD–Ppy nanoparticles

Magnetic Fe_3O_4 nanoparticles were prepared by the co-precipitation of Fe^{2+} and Fe^{3+} ions in ammonia solution and treatment under hydrothermal conditions (Shaw et al., 2006). Typically, 2.52 g of $FeCl_3 \cdot 6\,H_2O$ and 0.93 g of $FeCl_2 \cdot 4\,H_2O$ (molar ratio 2:1) were dissolved in 100 mL DI water under nitrogen atmosphere. Chemical precipitation was achieved by adding 10 mL of 26% NH_4OH solution at 25 °C under vigorous stirring. After incubation for 30 min at 80 °C, the resulting magnetite precipitates were separated by magnetic decantation and washed several times with DI water. Finally, the obtained Fe_3O_4 nanoparticles were dried by purging with nitrogen for 24 h and stored for future use.

The immobilization of GOD on Fe_3O_4 nanoparticles was performed by the following procedure. Fe_3O_4 nanoparticles (100 mg) were firstly introduced into a 2.5 mL EDC solution (2 mg mL^{-1}). The resultant suspension was sonicated for 6 min, and then 2.5 mL of GOD solution (3.0 mg mL^{-1}) was added. Subsequently, the mixture was sonicated sufficiently for 20 min and stored at 4 °C. After reaction for 2 h, the GOD-bound nanoparticles were recovered by placing the container on a strong permanent magnet, and then washed several times in DI water. Finally, the Fe_3O_4–GOD nanoparticles were freeze-dried and stored at 4 °C.

The GOD immobilized onto Fe_3O_4 nanoparticles was encapsulated by polymerization of pyrrole in 0.05 M phosphate buffer solution (PBS, pH 7.0) containing 3.0 mg mL^{-1} of Fe_3O_4–GOD, 15 mM of glucose and 150 mM of pyrrole. The glucose solutions were prepared at least 24 h before use and the polymerization reaction was performed at room temperature in air atmosphere. The polymerization of pyrrole was carried out for 6 h unless otherwise stated. Finally, the Fe_3O_4–GOD–Ppy nanoparticles were obtained and stored at 4 °C for use.

Modification of Fe_3O_4–GOD nanoparticles by polyaniline (PANI) layer was performed in terms of the method described previously (Kausaite-Minkstimiene et al., 2011), and Fe_3O_4–Ppy nanoparticles were prepared according to Yao′s protocol (Yao et al., 2013).

2.3. Fabrication of glucose biosensor

The MGCE was prepared according to Peng′s method with little modification (Peng et al., 2013). Briefly, paraffin oil (1.2 mL) was mixed with graphite powder (10 mg) thoroughly to get homogeneous paste. A copper wire was put into a Teflon tube (3 mm in diameter and 50 mm in depth) which was initially filled with a portion of the resulting paste, and a nummular magnet (3 mm in diameter and 2 mm in thickness, 0.2 T at the surface) was embedded with a depth of 2 mm from the surface of electrode. Then a glassy carbon (3 mm in diameter and 2 mm in depth) was inserted in the tube to immobilize the magnet and the edge of the glassy carbon was sealed by the adhesive. The prepared MGCE was carefully polished with 0.3 and 0.03 μm alumina slurries sequentially and then washed using DI water, followed by ultrasonic irradiation in ethanol–water solution and dried by air at room temperature. Subsequently, Fe_3O_4–GOD–Ppy aqueous suspension (0.5 mg mL^{-1}) was dripped onto the treated MGCE, the solid Fe_3O_4–GOD–Ppy nanoparticles were magnetically attracted down to the electrode surface immediately from the suspension, and the amount of Fe_3O_4–GOD–Ppy modified onto MGCE can be controlled and determined according to the volume changes of Fe_3O_4–GOD–Ppy aqueous suspension. The obtained Fe_3O_4–GOD–Ppy/MGCE biosensor was air-dried and kept at 4 °C when not in use.

2.4. Electrochemical measurements

The potentiometric response of the as-prepared glucose biosensor was performed in a two-electrode cell configuration with Fe_3O_4–GOD–Ppy/MGCE as the working electrode and Ag/AgCl as the reference electrode. All measurements were conducted in 5.0 mL solution at about 25 °C and the glucose concentrations were prepared in 0.1 M PBS (pH 6.0).

The sensing principle of the electrochemical glucose biosensor is based on an enzymatic reaction catalyzed by GOD according to the following equation:

$$\text{Glucose} + H_2O + O_2 \xrightarrow{\text{GOD}} \text{Gluconolactone} + H_2O_2$$

As a result of this reaction, gluconolactone and H_2O_2 are produced. The glucose can be detected through the two products and the oxygen consumption. Due to the presence of water, gluconolactone is spontaneously converted to gluconic acid, the charged species of gluconate and hydronium ions are generated as shown in the equation below:

$$\text{Gluconolactone} \xrightarrow{\text{spontaneous}} \text{gluconate}^- + H^+$$

This proteolytic reaction can be used for the determination of the glucose concentration (Shaw et al., 2003). Concentration changes of ions surrounding the Fe_3O_4–GOD–Ppy/MGCE will change the electrode potential.

3. Results and discussion

3.1. Preparation and characterization of the Fe_3O_4–GOD–Ppy/MGCE

The MGCE modified by Fe_3O_4–GOD–Ppy was fabricated as follows. As illustrated in Fig. 1, Fe_3O_4 nanoparticles were firstly prepared by co-precipitation of Fe^{2+} and Fe^{3+} ions in ammonia solution. Subsequently, the binding of GOD to Fe_3O_4 nanoparticles was accomplished via the reaction between a carboxyl group on the enzyme and an amine group on the nanoparticle surface (specifically, the C–O to C–N conversion) in the presence of EDC (Huang et al., 2003; Jordan et al., 2011). The resultant Fe_3O_4–GOD nanoparticles were mixed with the solution containing pyrrole and glucose, gluconic acid and H_2O_2 were generated by the catalytic reaction of GOD–glucose system, gluconic acid deceased the pH value, leading to optimal conditions for the H_2O_2 initiated polymerization of pyrrole (Ramanavičius et al., 2005; Ramanaviciene et al., 2006), self assembly of Ppy started on the surface of enzyme molecule under such favourable conditions and the core–shell Fe_3O_4–GOD–Ppy nanoparticles were successfully prepared. The obtained Fe_3O_4–GOD–Ppy nanoparticles were modified onto the MGCE surface, and then the glucose biosensor was fabricated.

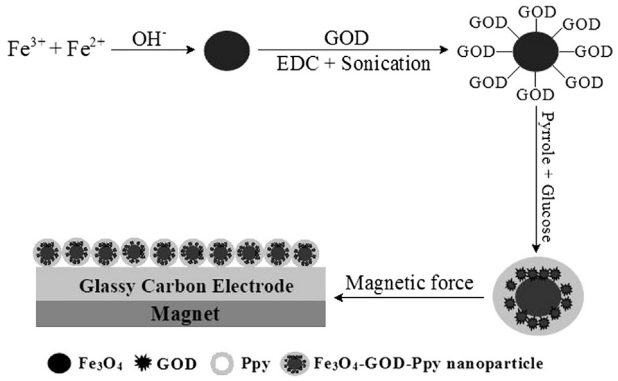

Fig. 1. Schematic illustration of the construction of Fe_3O_4–GOD–Ppy modified magnetic glassy carbon electrode.

TEM was employed to characterize the morphology and size of as-prepared Fe_3O_4–GOD–Ppy nanoparticles. As seen in Fig. 2A, the Fe_3O_4–GOD–Ppy nanoparticles are almost spherical or ellipsoidal and well dispersed, and these microspheres have an average diameter of about 48 nm, larger than the average diameter of 12.5 nm of the neat Fe_3O_4 nanoparticles, suggesting the encapsulation of GOD–Ppy on the surface of Fe_3O_4 nanoparticles and the formation of core–shell structure. The monodispersed characteristics of Fe_3O_4–GOD–Ppy nanoparticles can be related to the GOD–Ppy, which creates repulsive forces to balance the magnetic attractive forces and the van der Waals attractive forces of the magnetic nanoparticles and affect colloidal stability. The high dispersivity of these magnetic nanoparticles in solution is favorable for their immobilization to the MGCE surface. The structure of the resultant nanoparticles was characterized by FTIR spectra, as shown in Fig. 2B. In the FTIR spectrum of Fe_3O_4–GOD–Ppy, the peaks at 1554 and 1400 cm^{-1} refer to the fundamental vibration of the pyrrole rings (Liu and Wan, 2000), the bands observed at 1313, 1185 and 1046 cm^{-1} relate to the =C–H in-plane deformation vibration (Zhang et al., 2004), the =C–H out-of-plane bending vibration is found at 617 and 918 cm^{-1} (Bellamy, 1980), the peak at 573 cm^{-1} corresponds to the Fe–O stretching vibration of Fe_3O_4 (Chen et al., 2003), and the peak at 1654 cm^{-1} is attributed to C=O/C–N stretching vibration of amide I (Yang et al., 2008). Moreover, it was worth noting that the weak characteristic peak of Fe_3O_4 should be due to the presence of GOD–Ppy coating layer on Fe_3O_4, which further indicated that Fe_3O_4 nanoparticles were encapsulated inside GOD–Ppy shell. FTIR results strongly confirm the formation of core–shell Fe_3O_4–GOD–Ppy nanoparticles. Fig. 2C presents the magnetization curve of the nanoparticles measured at room temperature. A hysteresis loop was observed, indicating that the Fe_3O_4–GOD–Ppy nanoparticles were of ferromagnetic property. The nanoparticles exhibited a saturation magnetization (Ms) of 9.5 ± 0.3 emu g^{-1} and coercivity value (Hc) of 54 ± 4.8 Oe

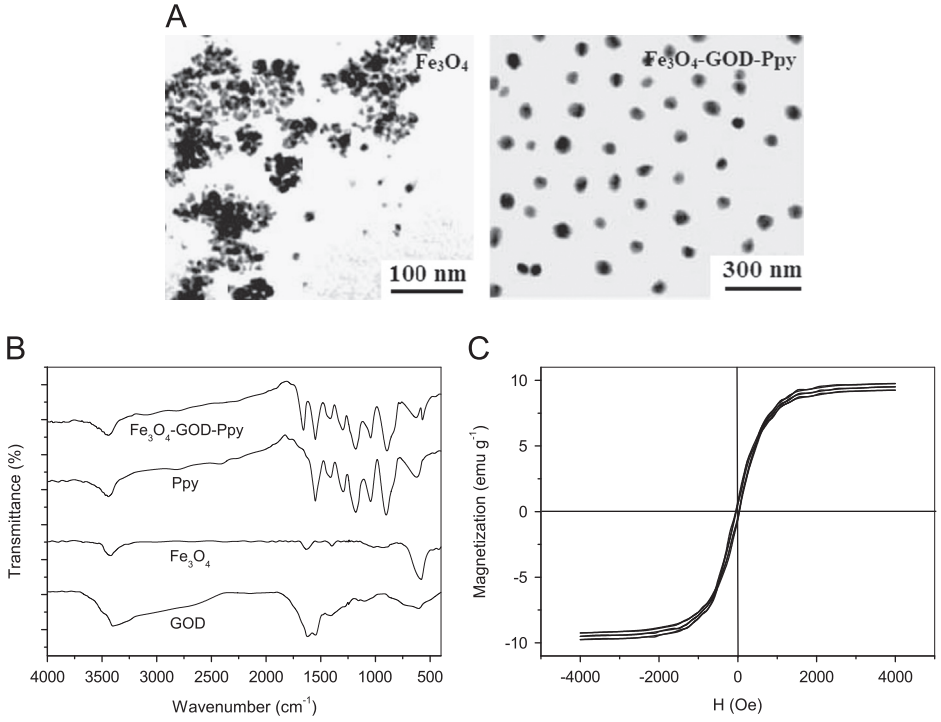

Fig. 2. TEM image (A), FTIR spectra (B), and magnetization curve (C) of synthesized Fe_3O_4–GOD–Ppy nanoparticles.

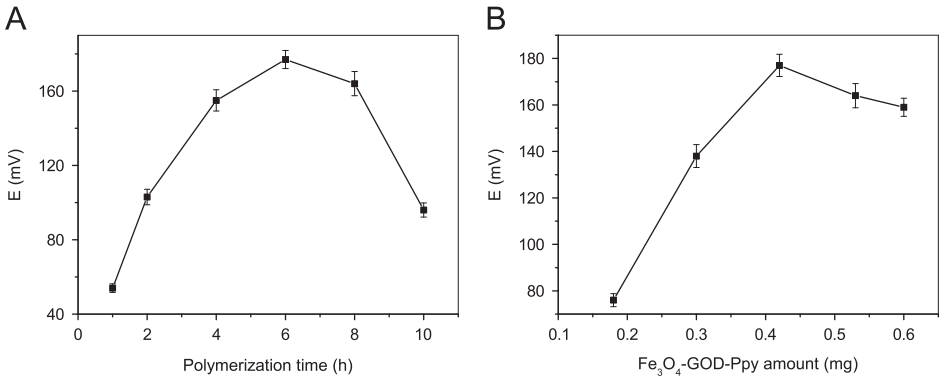

Fig. 3. Effects of Ppy polymerization time (A) and Fe_3O_4–GOD–Ppy amount modified on MGCE (B) on the response potential of glucose biosensor to 1.0 mM glucose in 0.1 M PBS (pH 6.0) at 25 °C. Average of three measurements (mean ± S.D.).

(mean ± S.D. $n=3$), which were quite different from the pure Fe_3O_4 nanoparticles with the Ms of 84 emu g^{-1} and Hc of 500–800 Oe (Yang et al., 2007). A reduction of Ms for Fe_3O_4–GOD–Ppy nanoparticles can be attributed to the presence of nonmagnetic GOD–Ppy shells, which decrease the magnetism of magnetic materials, whereas the low Hc may be resulted from the small size of Fe_3O_4 nanoparticles. In addition, it was worth noting that the remanence of the Fe_3O_4–GOD–Ppy nanoparticles was zero once the applied magnetic field was removed, indicating the superparamagnetic behavior of the nanoparticles. The results suggest that the obtained Fe_3O_4–GOD–Ppy nanoparticles possess excellent magnetic property, which is an advantage to their bioassay applications.

3.2. Optimization of biosensing conditions

In order to maximize the detection sensitivity of the Fe_3O_4–GOD–Ppy modified MGCE, the experimental conditions including the GOD immobilization on Fe_3O_4 nanoparticles, polymerization time of pyrrole and the immobilization amount of Fe_3O_4–GOD–Ppy on MGCE have been optimized. The response potential of glucose biosensor was performed in 1.0 mM glucose solution (pH 6.0) at 25 °C. Our experiments indicated that the saturation immobilization of GOD on Fe_3O_4 nanoparticles could be obtained after reaction for 2 h in 3.0 mg mL^{-1} enzyme solution at 4 °C. The response potential of the glucose biosensor depended on the polymerization time of pyrrole. As seen in Fig. 3A, the response potential increased with the increasing polymerization time from 1 to 6 h, and then decreased. Such phenomena can be closely related to Ppy amount in Fe_3O_4–GOD–Ppy nanoparticles, which increases with the increase in polymerization time (Ramanavičius et al., 2005). The Ppy modified at the surface of Fe_3O_4–GOD will be poor at a short polymerization time, the electron translation between Fe_3O_4–GOD–Ppy nanoparticles and MGCE may be inhibited and the enzyme activity may be decreased, causing a low potential response. However, the exorbitant Ppy content may hinder migration of glucose molecules into Fe_3O_4–GOD–Ppy nanoparticles and affect the binding of Fe_3O_4–GOD–Ppy nanoparticles on MGCE, resulting in a decrease of response potential at a long polymerization time. Therefore, Fe_3O_4–GOD–Ppy nanoparticles with polymerization time of pyrrole for 6 h were used to fabricate glucose biosensor. The electrical analysis indicated that the conductivity of the as-prepared Fe_3O_4–GOD–Ppy nanoparticles measured by standard four-probe method was 3.2×10^{-2} S cm^{-1}. Fig. 3B shows the effect of Fe_3O_4–GOD–Ppy amount modified on MGCE on the response potential of the glucose biosensor. The maximum response potential was observed when the Fe_3O_4–GOD–Ppy amount was increased to 0.42 mg, and then decreased gradually. Actually, the response potential depends on the GOD amount on MGCE and steric hindrance, the GOD amount will increase with the increasing Fe_3O_4–GOD–Ppy amount, showing an enhanced response potential. However, the higher immobilization amount of Fe_3O_4–GOD–Ppy on MGCE may hinder mass and electron transfer, causing a decrease in response potential. The relation between response potential and Fe_3O_4–GOD–Ppy amount suggest the optimal amount of Fe_3O_4–GOD–Ppy modified on MGCE is 0.42 mg.

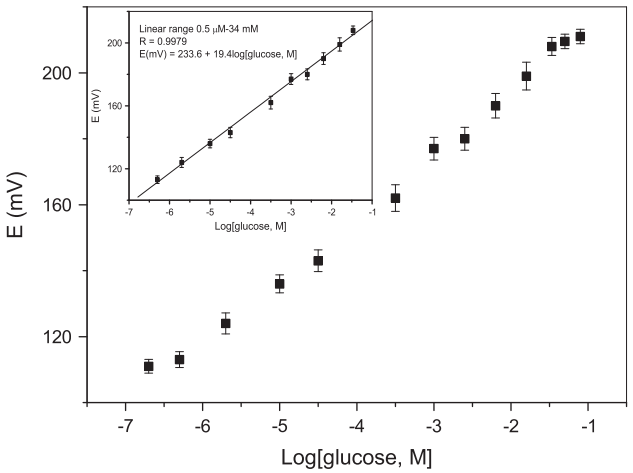

Fig. 4. Calibration graph obtained for the glucose biosensor in a glucose concentration range from 0.3 μM to 55 mM. The inset shows the linear part of the calibration graph. Average of three measurements (mean ± S.D.).

3.3. Biosensing performance

The dynamic range of the glucose biosensor was studied by monitoring the glucose solution in the concentration range from 0.3 μM to 55 mM. Fig. 4 presents the calibration curve between the response potential and the glucose concentration. A good linearity was observed in the wide concentration range (0.5 μM to 34 mM) (see the inset in Fig. 4). The linear regression equation was E (mV)=233.6+19.4 log[glucose, M], $R=0.9979$, $n=10$. The limit of detection (LOD), on basis of the definition by IUPAC ($C_{LOD}=3.3\ S_b\ m^{-1}$) (Irving et al., 1981), was found to be 0.3 μM, which was lower than that reported by other researchers (Çiftçi et al., 2013; Khun et al., 2012; Peng et al., 2013), indicating the high sensitivity of the sensor. The wide range of detection shown by the glucose biosensor can be attributed to the good enzyme loading capacity and large surface-to-volume ratio of Fe_3O_4–GOD–Ppy, which are favorable for oxidization of glucose molecules.

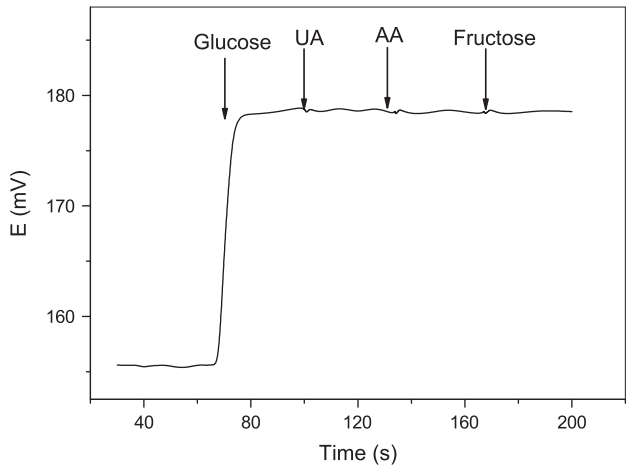

Fig. 5. Interference test protocols of the glucose biosensor to the interfering species (0.1 mM) in the presence of 1.0 mM glucose.

The selectivity of a glucose biosensor is closely related to the enzyme-analyte reaction and selective measurements. The enzyme-analyte reaction is very specific due to the nature of the glucose oxidase functionality. The glucose oxidase can only react with glucose because of its specific catalysis of glucose. In the work, some potential interferences such as uric acid (UA), ascorbic acid (AA) and fructose which were present in the human serum and well-known interferents with amperometric glucose oxidase methods were used to conduct the interference test, and the obtained results were shown in Fig. 5. As clearly seen from the output response of the sensor, a steady-state response potential reached within 6 s after addition of glucose into detector cell, the response signals of UA, AA, and fructose were essentially negligible, and no significant interference was observed upon the successive addition of 0.1 mM interferents into 1.0 mM glucose. These results suggest that the proposed Fe_3O_4–GOD–Ppy/MGCE has high selectivity, and the interfering species do not influence glucose determination.

The storage stability, or the ability of GOD to maintain activity over a long period of time, is an important aspect to be considered in the practical application of the glucose biosensor. To evaluate the long-term storage stability of the glucose biosensor, the operational stability of the Fe_3O_4–GOD–Ppy, Fe_3O_4–GOD–PANI, Fe_3O_4–GOD and Fe_3O_4–Ppy electrodes were investigated by the repeated measurements of analytical signals towards to 1.0 mM glucose within 20 days. Three consecutive measurements of 1.0 mM glucose were performed to get each point indicated in (Supplementary information Fig. S1). The electrodes were stored at 4 °C when not in use. The results obtained revealed that no obvious response potential was observed on Fe_3O_4–Ppy electrode (this is not shown in the graph). Potentiometric response of Fe_3O_4–GOD electrode decreased rapidly, leading to a poor stability. In contrast, Fe_3O_4–GOD–Ppy and Fe_3O_4–GOD–PANI electrodes exhibited a good stability, and response signals remained about 98.1% and 92.1% of their initial values after 20 days, respectively. Moreover, it was noted that Fe_3O_4–GOD–Ppy electrode was more stable than Fe_3O_4–GOD–PANI electrode. The excellent stability may be mainly attributed to the strong binding of Fe_3O_4–GOD–Ppy nanoparticles on MGCE and self-encapsulation of enzyme within Ppy, which improve resistance to leakage and denaturation of GOD molecules.

In order to demonstrate the feasibility of the glucose biosensor in real sample analysis, the biosensor was employed to measure glucose in human blood sample. The recovery test was performed by spiking with different concentrations of glucose to 5.0 mL serum sample and PBS. The serum samples were diluted 100 times before measurement and the obtained results were tabulated in Table 1 for comparison. The recoveries for the assays of 0.01–30.0 mM glucose in serum sample and PBS reached 97–100.8% and 98–100.3%, respectively, indicating that serum sample had no significant effect on glucose determination. The results indicate the glucose biosensor is feasible for practical analysis.

Table 1
The recovery determination of glucose in serum sample and PBS.

Added (mM)	Serum sample			PBS		
	Found (mM)		Recovery (%)	Found (mM)		Recovery (%)
	Mean[a]	R.S.D.[b](%)		Mean[a]	R.S.D.[b](%)	
0.01	0.0098	2.8	98	0.01	2.2	100
0.5	0.50	3.0	100	0.49	2.6	98
3.0	2.97	5.7	99	2.98	4.4	99.3
12.0	11.82	4.3	98.5	12.04	3.5	100.3
20.0	20.16	3.6	100.8	19.6	4.0	98
30.0	29.10	5.2	97	30.07	5.0	100.2

[a] Average of three determinations.
[b] Relative standard deviation.

4. Conclusions

TEM, FTIR and magnetization analysis confirmed the formation of core–shell Fe_3O_4–GOD–Ppy nanoparticles. A novel glucose biosensor was fabricated based on immobilization of Fe_3O_4–GOD–Ppy nanoparticles onto MGCE. The response of the biosensor was optimized and the optimal experimental conditions were polymerization time of pyrrole with 6 h and 0.42 mg immobilization amount of Fe_3O_4–GOD–Ppy nanoparticles on MGCE. Under the optimal conditions, the developed biosensor exhibited excellent activity and stability for the detection of glucose with a linear range from 0.5 μM to 34 mM, a low LOD (0.3 μM), fast response (6 s), high selectivity and stability.

Acknowledgements

This work was supported by the National Natural Science Foundation of China (No. 51202059), China Postdoctoral Science Foundation special funded project (No. 201104393), Key Research Project of Henan Province (No. 122102210120) and the Opening Project of Henan Key Discipline Open Laboratory of Mining Engineering Materials (No. MEM11-11).

Appendix A. Supporting information

Supplementary data associated with this article can be found in the online version at http://dx.doi.org/10.1016/j.bios.2013.07.054.

References

Bellamy, L.J., 1980. The Infrared Spectra of Complex Molecules, second ed. Chapman & Hall, London.
Chen, D., Deng, J., Liang, J., Xie, J., Hu, C.H., Huang, K.H., 2013. Sensors and Actuators B 183, 594–600.
Chen, D.H., Liao, M.H., 2002. Journal of Molecular Catalysis B 16, 283–291.
Chen, W., Li, X.W., Xue, G., Wang, Z.Q., Zou, W.Q., 2003. Applied Surface Science 218, 215–221.
Çiftçi, H., Tamer, U., Teker, M.Ş., Pekmez, N.Ö., 2013. Electrochimica Acta 90, 358–365.

Guo, C., Ma, Y.H., Su, P.F., Fang, B.S., 2012. Biochemical Engineering Journal 67, 120–125.
Hrapovic, S., Liu, Y., Male, K.B., Luong, J.H.T., 2004. Analytical Chemistry 76, 1083–1088.
Huang, S.H., Liao, M.H., Chen, D.H., 2003. Biotechnology Progress 19, 1095–1100.
Jordan, J., Kumar, C.S.S.R., Theegala, C., 2011. Journal of Molecular Catalysis B 68, 139–146.
Kalska-Szostko, B., Rogowska, M., Dubis, A., Szymański, K., 2012. Applied Surface Science 258, 2783–2787.
Kausaite-Minkstimiene, A., Mazeiko, V., Ramanaviciene, A., Ramanavicius, A., 2011. Sensors and Actuators B 158, 278–285.
Khun, K., Ibupoto, Z.H., Lu, J., Alsalhi, M.S., Atif, M., Ansari, A.A., Willander, M., 2012. Sensors and Actuators B 173, 698–703.
Kim, J., Grate, J.W., 2003. Nano Letters 3, 1219–1222.
Kim, J.H., Lim, S.Y., Nam, D.H., Ryu, J., Ku, S.H., Park, C.B., 2011. Biosensors and Bioelectronics 26, 1860–1865.
Kim, S.H., Kim, M.J., Choa, Y.H., 2007. Materials Science and Engineering A 449-451, 386–388.
Kotanen, C.N., Moussy, F.G., Carrara, S., Guiseppi-Elie, A., 2012. Biosensors and Bioelectronics 35, 14–26.
Kotanen, C.N., Tlili, C., Guiseppi-Elie, A., 2013. Talanta 103, 228–235.
Liang, B., Fang, L., Yang, G., Hu, Y.C., Guo, X.S., Ye, X.S., 2013. Biosensors and Bioelectronics 43, 131–136.
Liu, J., Wan, M.X., 2000. Journal of Polymer Science Part A: Polymer Chemistry 38, 2734–2739.
Mahmood, I., Ahmad, I., Chen, G., Liu, H.Z., 2013. Biochemical Engineering Journal 73, 72–79.
Pang, X., He, D., Luo, S., Cai, Q., 2009. Sensors and Actuators B 137, 134–138.
Pasunooti, S., Surya, W., Tan, S.N., Liang, Z.X., 2010. Journal of Molecular Catalysis B 67, 98–103.
Peng, H.P., Liang, R.P., Qiu, J.D., 2011a. Biosensors and Bioelectronics 26, 3005–3011.
Peng, H.P., Liang, R.P., Zhang, L., Qiu, J.D., 2011b. Electrochimica Acta 56, 4231–4236.
Peng, H.P., Liang, R.P., Zhang, L., Qiu, J.D., 2013. Biosensors and Bioelectronics 42, 293–299.
Qiu, J.D., Peng, H.P., Liang, R.P., Xia, X.H., 2010. Biosensors and Bioelectronics 25, 1447–1453.
Ramanaviciene, A., Schuhmann, W., Ramanavičius, A., 2006. Colloids and Surfaces B 48, 159–166.
Ramanavičius, A., Kaušaitė, A., Ramanavičienė, A., 2005. Sensors and Actuators B 111–112, 532–539.
Ramanavičius, A., Ryskevic, N., Kausaite-Minkstimiene, A., Bubniene, U., Baleviciute, I., Oztekin, Y., Ramanaviciene, A., 2012. Sensors and Actuators B 171-172, 753–759.
Shaw, G.W., Clarement, D.J., Pickup, J.C., Bergveld, P., 2003. Analyst 128, 1062–1066.
Shaw, S.Y., Chen, Y.J., Ou, J.J., Ho, L., 2006. Enzyme and Microbial Technology 39, 1089–1095.
Snyder, S.L., McAuley, K.B., McLellan, P.J., Brouwer, E.B., McCaw, T., 2011. Sensors and Actuators B 156, 621–630.
Tan, Y.M., Deng, W.F., Chen, C., Xie, Q.J., Lei, L.H., Li, Y.Y., Fang, Z.F., Ma, M., Chen, J.H., Yao, S.Z., 2010. Biosensors and Bioelectronics 25, 2644–2650.
Vijayalakshmi, A., Tarunashree, Y., Baruwati, B., Manorama, S.V., Narayana, B.L., Johnson, R.E.C., Rao, N.M., 2008. Biosensors and Bioelectronics 23, 1708–1714.
Wang, S.F., Tan, Y.M., Zhao, D.M., Liu, G.D., 2008. Biosensors and Bioelectronics 23, 1781–1787.
Wei, H., Wang, E., 2008. Analytical Chemistry 80, 2250–2254.
Wu, S., Wang, H.N., Tao, S.Y., Wang, C., Zhang, L.H., Liu, Z.G., Meng, C.G., 2011. Analytica Chimica Acta 686, 81–86.
Xia, W.L., Ma, N., 2010. Biomass and Bioenergy 34, 890–896.
Yan, M., Ge, J., Liu, Z., Ouyang, P.K., 2006. Journal of American Chemical Society 128, 11008–11009.
Yang, H.Y., Jiang, W., Lu, Y., 2007. Materials Letters 61, 2789–2793.
Yang, Z.P., Si, S.H., Zhang, C.J., 2008. Biochemical and Biophysical Research Communications 367, 169–175.
Yao, T.J., Cui, T.Y., Fang, X., Yu, J., Cui, F., Wu, J., 2013. Chemical Engineering Journal 225, 230–236.
Zhang, X.T., Zhang, J., Liu, Z.F., Robinsion, C., 2004. Chemical Communications 10, 1852–1853.
Zhang, Z.X., Wang, Z.J., Wang, X.L., Yang, X.R., 2010. Sensors and Actuators B 147, 428–433.
Zhao, G., Xu, J.J., Chen, H.Y., 2006. Electrochemistry Communications 8, 148–154.
Zhao, H.T., Ju, H.X., 2006. Analytical Biochemistry 350, 138–144.
Zhou, H.C., Li, W., Shou, Q.H., Gao, H.S., Xu, P., Deng, F.L., Liu, H.Z., 2012. Chinese Journal of Chemical Engineering 20, 146–151.
Zou, C., Fu, Y.C., Xie, Q.J., Yao, S.Z., 2010. Biosensors and Bioelectronics 25, 1277–1282.